Proof-of-Concept of Dedicated Aerial 5G and GNSS Testbed for Enhanced Hybrid Positioning

José A. del Peral-Rosado (1), Patric Nolle (1), Fabian Rothmaier (1), Sara M. Razavi (2), Gustav Lindmark (2), Xiaolin Jiang (2), Deep Shrestha (2), Fredrik Gunnarsson (2), Sagar Parsawar (3), Rakesh Mundlamuri (3), Florian Kaltenberger (3), Niilo Sirola (4), Olli Särkkä (4), Uzair A. Noman (4), Juha Roström (4), Kim Vaarala (4), Pasi Miettinen (4), Stefano Garlaschi (5), Luca Canzian (5), Huseyin Babaroglu (6), Elizaveta Rastorgueva-Foi (6), Matias Turunen (6), Jukka Talvitie (6), Detlef Flachs (1)

(1) *Airbus Defence and Space, Taufkirchen, Germany*
(2) *Ericsson Research, Linköping, Sweden*
(3) *Eurecom, Sophia-Antipolis, France*
(4) *Exafore, Tampere, Finland*
(5) *Qascom, Bassano del Grappa, Italy*
(6) *Tampere University, Tampere, Finland*

BIOGRAPHY

José A. del Peral-Rosado is a Senior Navigation Engineer at Airbus Defence and Space GmbH.
Patric Nolle is a Senior Navigation engineer at Airbus Defence and Space GmbH.
Fabian Rothmaier is a R&D Navigation Engineer at Airbus Defence and Space GmbH.
Sara M. Razavi is Master Researcher at Ericsson Research.
Gustav Lindmark is Senior Researcher at Ericsson Research.
Xiaolin Jiang is Experienced Researcher at Ericsson Research.
Deep Shrestha is Senior Researcher at Ericsson Research.
Fredrik Gunnarsson is an Expert in RAN Automation and Positioning at Ericsson Research.
Sagar Parsawar is a Research Engineer at Eurecom.
Rakesh Mundlamuri is a PhD Student at Eurecom.
Florian Kaltenberger is an Assistant Professor in the Communication System department at Eurecom.
Niilo Sirola is a Principal Specialist at Exafore.
Olli Särkkä is a Senior Specialist at Exafore.
Uzair A. Noman is a Senior Software Engineer at Exafore.
Juha Roström is the CEO at Exafore.
Kim Vaarala is a Technical Project Manager at Exafore.
Pasi Miettinen is a Senior Software Engineer at Exafore.
Stefano Garlaschi is a R&D Navigation Engineer at Qascom.
Luca Canzian is the Head of the R&D unit at Qascom.
Huseyin Babaroglu is a Research Assistant at Tampere University.
Elizaveta Rastorgueva-Foi is a PhD student at Tampere University.
Matias Turunen is a Specialist at Tampere University.
Jukka Talvitie is an University Lecturer at Tampere University.
Detlef Flachs is the Head of Germany Future Navigation Programs department at Airbus Defence and Space GmbH.

DISCLAIMER

The view expressed herein can in no way be taken to reflect the official opinion of the European Space Agency.

ABSTRACT

This work presents the preliminary simulation and experimental results of a first-of-a-kind testbed for GNSS, 5G networks and sensor positioning, called Hybrid Overlay Positioning with 5G and GNSS (HOP-5G) testbed. This is a proof-of-concept testbed

based on the deployment of dedicated ground and aerial 5G base stations (BSs) for enhanced hybrid positioning together with GNSS and sensor technologies. The main entities of the overall testbed are described and preliminary test results are provided. First, the achievable positioning performance is assessed through simulations, showing the importance of the hybrid fusion of GNSS and 5G in critical and harsh environments, especially under 5G network synchronization impairments. Then, the possible gain in integrity performance is examined by fusing real GNSS and simulated 5G observables. Finally, extensive experimental laboratory results are presented to assess the impact of base station (BS) synchronization, by using COTS GNSS and software-defined radio (SDR) equipment. The outcome results suggests the importance of a monitoring unit within the HOP-5G testbed.

1. INTRODUCTION

Cellular communication signals have been used for positioning from early generations, as it is reviewed in del Peral-Rosado et al. (2018a). However, the achievable accuracies have been never sufficient for vehicular or aerial applications. Indeed, there is a need for accurate and timely positioning on safety-critical automotive and aerial applications, as it is reported in 3GPP TR 22.872 (2018), such as advance warning systems and vulnerable road user protection, airspace management with high traffic capacities or in urban air mobility. Today, these high-accuracy demands can partially be satisfied by Global Navigation Satellite Systems (GNSS), though not in dense urban conditions and other challenging situations. In order to achieve increased positioning performance especially in these challenging environments, a first-of-a-kind testbed is presented for hybrid 5th Generation (5G) network and GNSS positioning (together with sensor fusion), called Hybrid Overlay Positioning with 5G and GNSS (HOP-5G) testbed. The core idea of the HOP-5G testbed is to utilize the new 5G mobile signals to support accurate 3D position and motion information, especially for challenging urban and suburban scenarios. This testbed is particularly timely, as its development coincides with the end of 3GPP Release 17 work in 3GPP TR 38.857 (2021) and the start of 3GPP Release 18 standardization activities, as it is planned in RP-213588 (2021). In this context, hybrid positioning using temporary and dynamic deployment of 5G overlay networks in combination with GNSS is expected to be suitable for a wide range of application areas, as it is early discussed in del Peral-Rosado et al. (2022). Moreover, such dedicated deployment may provide learnings in terms of the Radio Access Technology (RAT)-dependent integrity framework, which is part of the 3GPP Release 18 positioning study scope.

To the best of authors knowledge, the HOP-5G testbed is expected to be one of the first field demonstrators of hybrid 5G and GNSS positioning capabilities over aerial vehicles, when using a dedicated deployment and standard-compliant 3GPP 5G signals. The preliminary results of this paper provide insights on the expected positioning performance with dedicated 5G networks, under outdoor and aerial conditions. These are complementary to existing 3GPP simulation results in 3GPP TR 38.857 (2021), hybrid GNSS and cellular evaluations in del Peral-Rosado et al. (2017, 2018, 2019), predecessor hybrid GNSS and 5G testbeds in Maymo-Camps et al. (2018); Mata et al. (2020), and 5G opportunistic or signals-of-opportunity studies in Shamaei & Kassas (2021); Abdallah & Kassas (2021). These results are based on the exploitation of 5G signals together with GNSS and sensor measurements. This proof-of-concept is expected to demonstrate a new dimension in terms of provision of on-demand positioning capabilities, such as thanks to dedicated flying 5G base stations.

2. HOP-5G TESTBED ARCHITECTURE

The HOP-5G testbed is organized in five general blocks, as it is shown in the high-level testbed architecture in Figure 1. The Ground Support Equipment (GSE) is in charge of the control, command, data collection, monitoring and post-processing functionalities of the testbed. The testbed operator uses the interface within GSE to command and monitor the HOP-5G testbed. Then, the 5G base stations (BSs) or gNodeBs (gNBs) can be deployed at fixed locations on ground and at movable locations, such as on ground vehicles or on the payload of unmanned aerial vehicles (UAVs). Finally, the 5G BSs and/or User Equipment (UE) perform measurements from multi-constellation GNSS, 5G and sensors, in order to compute the stand-alone or hybrid positioning of the UE targeting real-time operation.

2.1. GROUND SUPPORT EQUIPMENT

The GSE is used to command and control the testbed, and to support the exchange of information among the different modules. It also includes data-storage capabilities, post-processing functions and testbed operator interface:

- **Monitoring unit**: the 5G monitoring unit is collocated with the UE, and it is used to estimate possible synchronization offsets among the BSs and to provide the associated time corrections to the UE. These corrections are used to improve the UE positioning, especially of time-difference of arrival (TDoA) methods, either in real-time or through a post-processing analysis. The monitoring unit contains software module in charge of estimating the 5G BS time offset from the received processed signals, by considering the 5G BS positions and the UE reference position (within the testbed).

- **Storage and post-processing unit**: This unit is in charge of performing the necessary post-processing of the data collected (including I/Q samples, measurements and results), as well as performance assessments. This unit can run the 5G offline processing module and the hybrid positioning algorithms.
- **Testbed operator interface**: This is the interface for the control and command of the testbed functionalities and monitoring of the general status (including UAV operations).

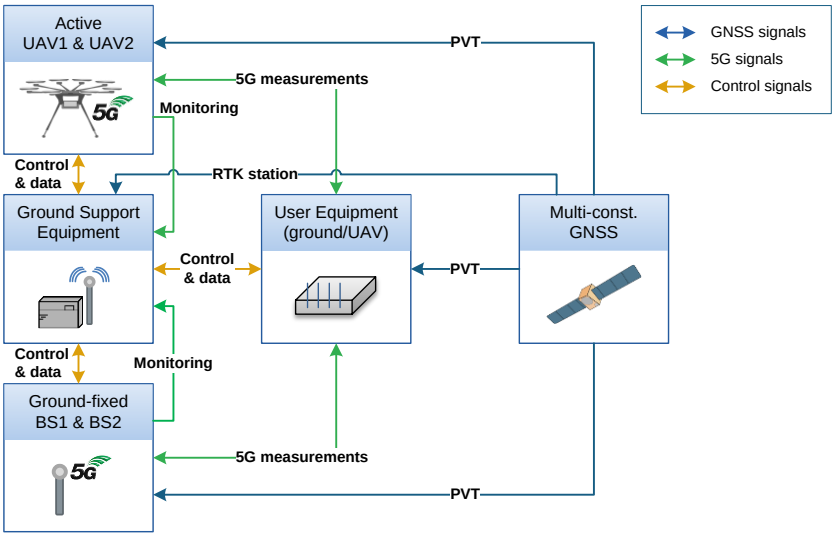

Figure 1 *High-level HOP-5G testbed architecture*

2.2. 5G BASE STATIONS

The 5G BSs establish the transmission and reception of 5G signals with the UE. Each BS includes a COTS GNSS receiver with Real-Time Kinematics (RTK) capabilities for precise positioning and time synchronization, a control and data unit to exchange information (e.g., RTK corrections) with other modules, a 5G software-defined radio (SDR) to transmit and/or receive in frequency range 1 (FR1), i.e., below 6 GHz, and 5G and GNSS antennas. Additional mmWave equipment (controlled through SDR FR1 equipment or on-board computer) is used to transmit and/or receive in FR2, i.e., above 24 GHz. This mmWave equipment is proposed as baseline to be located on the ground-fixed BSs, and additionally integrated in the payload of one UAV BS. The on-board computer (OBC) can execute (through the SDR block) the 5G real-time processing module at BS, i.e., based on the OpenAirInterface (OAI), being able to store signal samples, to receive 5G signals, and to transmit 5G generated in real-time or pre-generated. The 5G BS measurements can be temporary collected in the OBC and transferred to the GSE and UE targeting real-time. Two types of base stations are envisaged:

- **Ground-fixed BS**: the BS is located at a fixed position on ground.
- **UAV BS (or active UAV)**: the BS is integrated in a UAV, which includes additional sensors to the GNSS receiver.

2.3. USER EQUIPMENT

The UE includes the hybrid positioning solutions considered within the HOP-5G testbed, which are executed in the OBC. It may be placed on a fixed or movable platform (e.g., a pedestrian or a drone). It contains the same building blocks as a BS, but also includes additional sensors. The OBC can also execute (through the SDR block) the 5G real-time processing module at UE (i.e., OAI UE) to transmit and receive 5G signals, being able to store signal samples, or to transmit 5G uplink pre-generated signals. Additional mmWave equipment (controlled through SDR FR1 equipment or on-board computer) is used to transmit and/or receive in FR2. It is remarked that within the UE two types of positioning solutions are computed:

- **Hybrid solution**: the hybrid positioning solution considered in the testbed is computed using the information extracted from the 5G signals, the GNSS data without the application of the RTK corrections, and the sensor data. For a UAV UE, the barometric and inertial measurement unit (IMU) information is of special interest for the hybrid solution.
- **Reference solution**: the reference position and trajectory of the UE that is provided to the system in real-time or post-processing, used to assess the accuracy of the hybrid solution. This reference is based on the GNSS RTK solution with any additional sensor data if available, while this can be enhanced with a tachymeter for further assessment purposes.

3. ASSESSMENT OF POSITIONING PERFORMANCE

3.1. GENERAL POSITIONING PERFORMANCE

This section aims at providing an assessment on the performance of different positioning methods for the HOP-5G testbed, based on the 3GPP simulation methodology in 3GPP TR 38.855 (2019). The simulations on FR1 are done for a maximum bandwidth of 100MHz, while the ones for FR2 are with a maximum bandwidth of 400MHz. Bandwidth is one of the main parameters that impacts the measurement accuracy, and hence if we keep the same bandwidth of FR1 in FR2, then we can expect similar positioning performance. These simulations consider ranging-based positioning methods, including downlink TDoA (DL-TDoA), uplink TDoA (UL-TDoA) and multi-round-trip-time (Multi-RTT). These methods are described in 3GPP TS 38.305 (2020) and discussed in Dwivedi et al. (2021). The simulated deployment considers four BSs with omnidirectional antennas for FR1 and directional antennas for FR2 at each corner of a rectangular deployment of 200m x 200m, as it is shown in Figure 2. In this simulation study, no interference has been considered, meaning that in terms of downlink, one can imagine a perfect muting scenario in which no Positioning Reference Signal (PRS) from neighbor cells adds any interference on the PRS of the other cells, and in case of uplink, no SRS from UEs in the same area create interference towards other UEs.

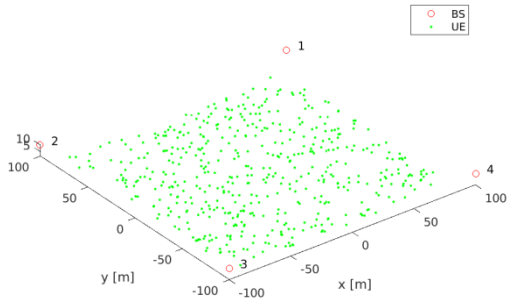

Figure 2 *Dedicated network based on 4 BSs with outdoor UEs uniformly and centrally distributed in a 200m x 200m area*

With this simulation setup, and the availability of ranging measurements, the performance of all three ranging-based methods (i.e. DL-TDoA, UL-TDoA and Multi-RTT) are very similar to each other, as it is shown in Figure 3 (left). However, if the network synchronization error is considered, then Multi-RTT is expected to result in a better performance, thanks to the clock synchronization through transmission and reception timestamps of the two-way communication. An important factor that significantly impacts the positioning performance is the availability of line-of-sight (LoS) links or not. According to Figure 3 (left), in the best case scenario, in which all four BSs have LoS links to the UE, the UEs the positioning accuracy is below 50cm in FR1 (99% confidence level). Note that this result is based on 2D search and the vertical positioning has not been considered. Moreover, by extending the simulation work to FR2 with 400MHz, the positioning accuracy significantly improves. Figure 3 (right) illustrates that the positioning accuracy is expected to be almost below 5cm for more than 99% of the cases for almost all the three ranging-based positioning methods. Again one should note that these are the ideal scenarios with perfect network synchronization to assess the technology potentials of 5G, but they should be not directly considered as benchmarking evaluation for the HOP-5G testbed, since additional performance impairments are expected with field experimentation.

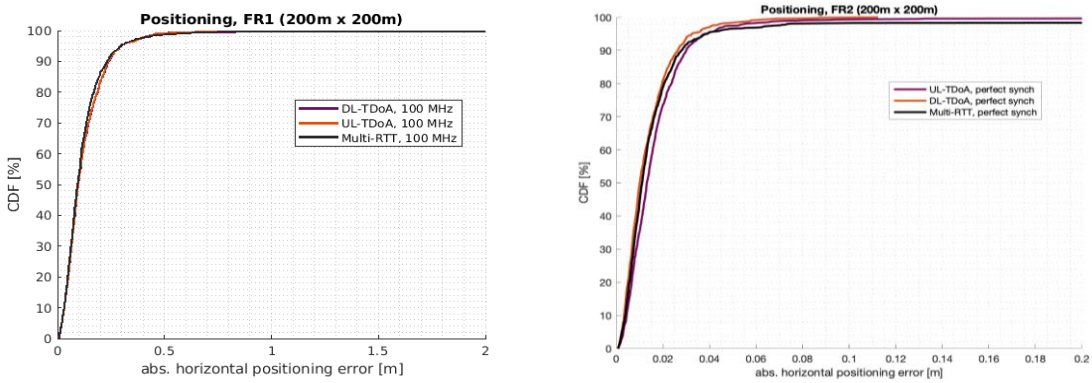

Figure 3 *Positioning performance of DL-TDoA, UL-TDoA and Multi-RTT in FR1 (left) and in FR2 (right)*

3.2. BENCHMARKING OF FIELD TESTING

In order to evaluate future field test performance results, the setup of test scenarios have been simulated in the Ericsson internal positioning simulation tool, and by tuning all the parameters according to the future field tests, a proper benchmarking system is in place. In the following subsections, first details of the scenarios are described and then all the simulations results are provided to show the impact of each network factor on the positioning accuracy.

TEST SCENARIOS. Four scenarios are defined with four deployed BSs and one UE over the future field test area. Two of these BSs are fixed on the ground and two of them are at UAVs, which have the potential to be at different heights. Both UE on the ground and at UAV with flying trajectory are studied in these scenarios. Table 1 provides the details of these four scenarios. Note that the UAV height of BS3 and BS4 has been optimized to achieve the best vertical positioning accuracy.

TABLE 1

Field test scenario descriptions `

Scenario	**BS1**, latitude: 48.047606°, longitude: 11.653582°	**BS2**, latitude: 48.047793°, longitude: 11.653843°	**BS3**, latitude: 48.048341°, longitude: 11.653843°	**BS4**, latitude: 48.048390°, longitude: 11.654665°	**UE**
1	On heliport tower, height: 9m	On ground, height: 1.5m	On ground, height: 1.5m	On ground, height: 1.5m	On ground
2					On UAV
3			On UAV, height: 10m	On UAV, height: 60m	On ground
4					On UAV

Figure 4 (left) provides an illustration of the field test simulation area with the location of the BSs and the UAV trajectory from top view. For simulating the UAV flying trajectory, the UE on ground is provided with a random UE position over the circle area defined by the UAV flying trajectory shown in Figure 4 (right). The movement starts with 10m up vertically and then spiral up to 60m followed by several orbits at 60m and then spiral back down.

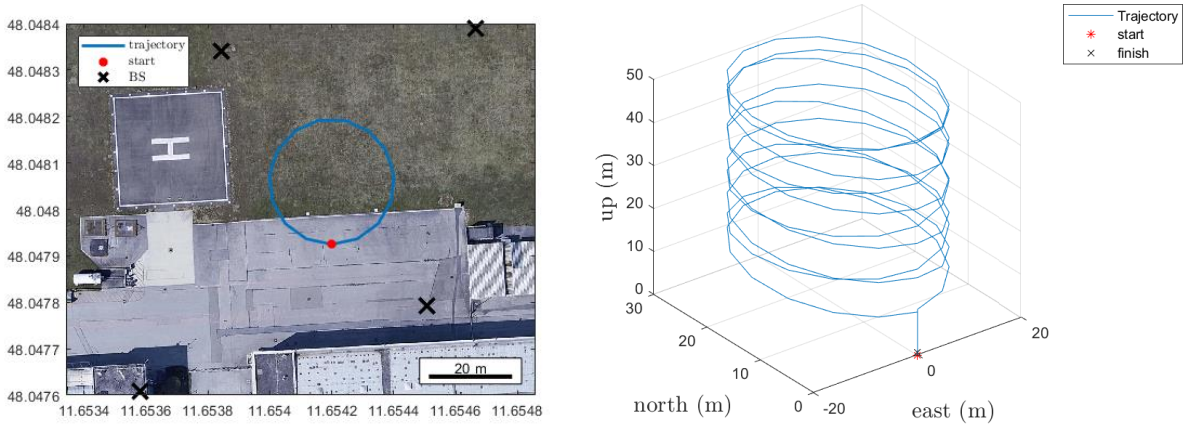

Figure 4 *Simulation setup of the field test (left) and the simulated UAV flying trajectory (right)*

SIMULATION RESULTS. The DL-TDOA method has been used for benchmarking the achievable 5G positioning accuracy with 23dBm transmit power at the BSs and the PRS bandwidth of 80MHz. An ideal synchronized scenario is assumed meaning that the synchronization error between BSs is 0ns. For all 5G simulations, the urban micro (UMi) channel model is used, based on 3GPP TS 38.901 (2019). Moreover, an Extended Kalman Filter (EKF) is used to track the UE for all simulations in this section.

The performance of the DL-TDOA method is shown in Figure 5 for each of the scenarios defined in Table 1. The altitude of UAV BSs 3 and 4 are tuned to 10m and 60m, respectively, in order to achieve the best positioning performance. Indeed, this implies that the BSs do not align on one geometrical plane, hence improving the triangulation of DL-TDoA result. Moreover, as the UE is flying up to 60m, it is important that one of the BSs cover that height. All scenarios are first evaluated under the assumption that the UE height is known, which basically results in a 2D position estimation problem. Then, 3D positioning estimation is done for

scenarios 2 and 4, which have a UAV UE with flying trajectory. Both 3D positioning cases result in much worse positioning performance, due to the constrained positioning problem. In the worse-case scenario, which is Scenario 2, the positioning error is still well below 3m during more than 90% of the trajectory. One should observe that the performance of Scenario 1 is well aligned with what has been studied for 5G standardization work, with accuracy of less than 50cm for 90% of the cases.

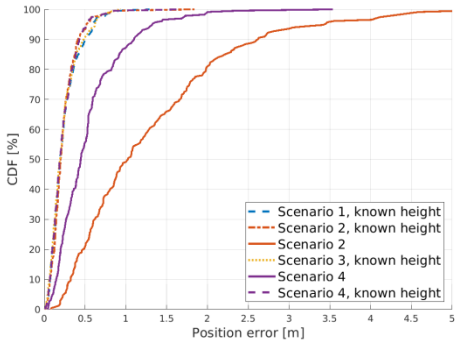

Figure 5 *Nominal DL-TDoA performance for Scenarios 1, 2, 3 and 4*

The rest of the simulation studies from this section focus on Scenario 4, which considers two UAV BSs and one UAV flying trajectory as a UE, resulting in the most challenging and interesting setup for this field test benchmarking. In the next step, the bandwidth comparison in 5G FR1 is shown in Figure 6 (left). The transmission (Tx) power is set to 23dBm and no synchronization error is considered. As expected, we can observe that an increase of the bandwidth results in a significant improvement in the positioning performance. While from 5G perspective, it is possible to consider a bandwidth up to 100MHz in FR1, we limited this comparison in the scale of the testbed values with 20, 40 and 80MHz.

The next parameter to evaluate is the Tx power of the PRS signals from the BSs. In Figure 6 (center), the Tx power is set to 0dBm, 10dBm and 23dBm for Scenario 4. The bandwidth is 80MHz and perfect BS synchronization is assumed. The figure shows that with line-of-sight conditions and relatively nearby BSs, the Tx power is not impacting the positioning performance. Note that the simulation outcome is driven by the urban micro (UMi) channel model, thus field test results are of special interest in this aspect.

The synchronization error is the next parameter to consider. The bandwidth and the Tx power are set to 80MHz and 23dBm, respectively, for Scenario 4. BS synchronization errors of 20ns and 50ns are compared with the ideal synchronization case (i.e., 0ns). Figure 6 (right) illustrates the positioning performance of these three cases. The results show the significant impact of the synchronization in the positioning accuracy. Note that for the cases with synchronization errors, the same errors are used for the complete UE trajectory. Therefore, they result in a position estimation error at all positions on the trajectory. The impact of this error is much higher compared to the impact of the previous parameters, this makes the DL-TDOA method vulnerable to this error.

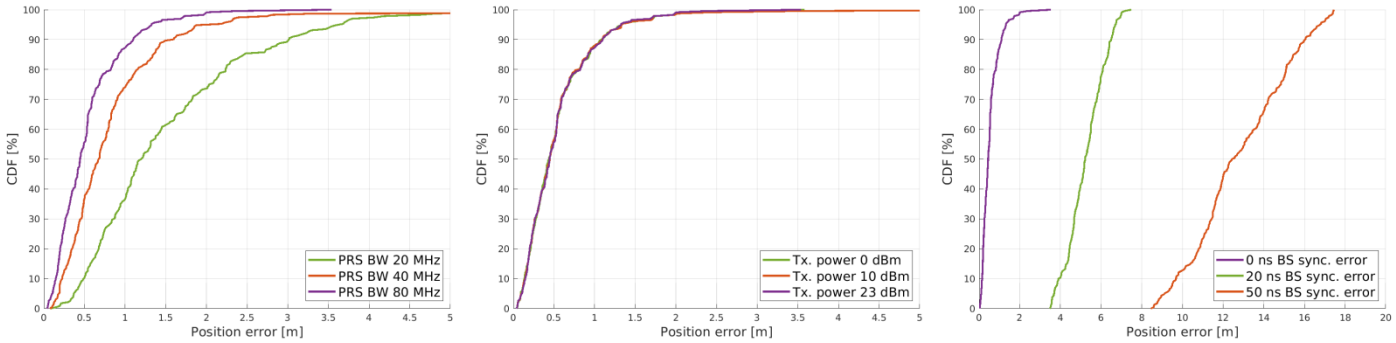

Figure 6 *Impact evaluation of bandwidth (left), transmit power (center) and synchronization error (right) on positioning performance of Scenario 4*

One main goal of the field study is to explore the hybrid 5G and GNSS positioning potentials. This is here assessed by comparing the performance of 5G positioning with respect to hybrid 5G and GNSS positioning, under nominal and degraded operational conditions of each technology. These operational conditions are defined as follows:

- **Nominal 5G**: 0ns synchronization error, 80 MHz bandwidth, 23 dBm Tx power;
- **Degraded 5G**: 20 ns synchronization error, 40 MHz bandwidth, 0 dBm Tx power;
- **Nominal GNSS**: open-sky scenario with only GPS and Galileo constellations;
- **Degraded GNSS**: elevation mask of 60° applied to open-sky scenario with only GPS and Galileo constellations.

The hybrid positioning solution is implemented with an EKF, and no sensor information is considered for this hybrid solution. Four options are compared with each other for Scenario 4:

- Option 1: Nominal 5G
- Option 2: Hybrid GNSS + Nominal 5G
- Option 3: Degraded 5G
- Option 4: Hybrid GNSS + Degraded 5G

Considering nominal GNSS conditions, these four options (of Scenario 4) are simulated as shown in Figure 7 (left). The improvement in positioning performance when adding GNSS in the hybrid solution is visible, while in the case of degraded 5G scenario, the scale of the improvement is significant moving from 6m positioning error in 80% of the cases to much below 1m.

Considering degraded GNSS conditions, the previous four options are once again compared with each other for Scenario 4. Figure 7 (right) shows that hybrid 5G and GNSS solutions would significantly improve the positioning estimation of a degraded 5G network, and this is even true for the case in which the GNSS has degraded capabilities, i.e., with a reduction of the number of available satellites.

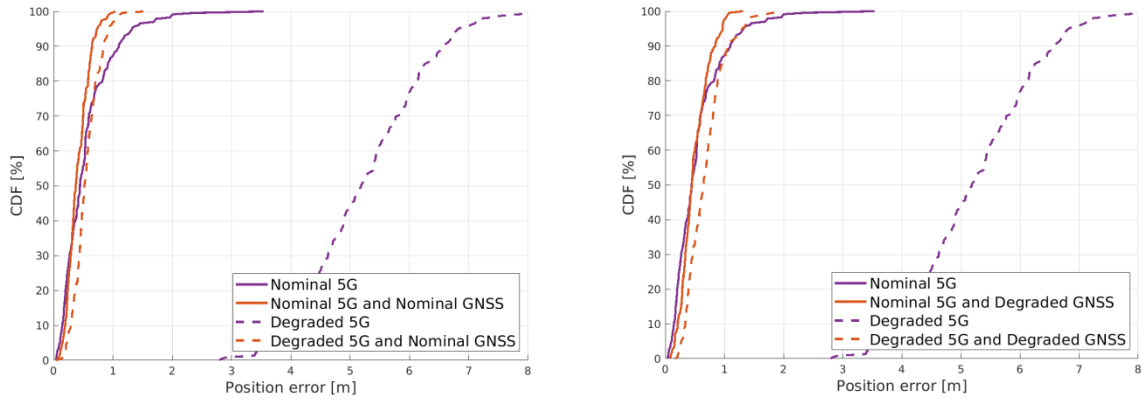

Figure 7 *Hybrid GNSS and 5G positioning performance under nominal/degraded 5G and nominal GNSS conditions (left) and under nominal/degraded 5G and degraded GNSS conditions (right)*

The setup may not be ideal for a 5G positioning evaluation, and especially the fact that DL-TDoA has been used as the 5G positioning method with very few BSs. It is worth mentioning that 5G angular and multi-RTT methods are robust to BS synchronization errors. Therefore, they are expected to provide better 5G positioning performance for the considered scenarios. However, the intention of this study is to showcase and justify the importance of hybrid positioning and fusion of GNSS and 5G for positioning performance in critical and harsh environments.

3.3. ASSESSMENT OF POSITIONING INTEGRITY

This section analyses the potential use of 5G measurements for integrity. Specifically, the additional measurements are leveraged at the user level to compute protection levels (PLs). We follow the approach known as Receiver Autonomous Integrity Monitoring (RAIM), where the redundancy of measurements is leveraged to provide a guarantee on the positioning error. A detailed description of the concept goes beyond the scope of this paper – the interested reader is referred to Parkinson & Axelrad (1988) for the original concept and Blanch et al. (2014) for the Advanced RAIM (ARAIM) framework used within this paper.

The cited Multi-Hypothesis-Solution-Separation (MHSS) ARAIM algorithm is a snapshot integrity algorithm based on GPS and Galileo measurements. Several improvements have been suggested w.r.t. the baseline algorithm, such as in Blanch, J. and Walter, T. (2021) and Blanch, J. et al. (2022). Improved performance can further be achieved using sequential approaches to exploit satellite motion (Joerger, M. and Pervan, B. (2016)), using a Kalman Filter (Joerger, M. and Pervan, B. (2013)) or banks of filters as by Gunning, K., et al. (2018) and Wendel, J. (2018).

The point of this study however is not to compute the tightest possible protection level. It is rather to examine the possible gain in performance by including 5G signals together with GNSS, given certain assumptions about 5G measurement models and fault rates. The results will be strongly dependent on these assumptions, and therefore have to be interpreted on a qualitative basis. The baseline snapshot ARAIM algorithm is therefore chosen as a basis for implementation, as it provides a relatively consolidated baseline while limiting the complexity of the algorithm.

Similar work has been conducted in Maaref, M., Khalife, J., and Kassas, Z. M. (2021) for signals of opportunity and with simplified measurement fault assumptions. Specifically, in this work we do not limit the MHSS algorithm to consider only single fault hypothesis but consider the full range of hypothesis resulting from the assumed fault probabilities of each satellite constellation and the 5G measurements.

ALGORITHM IMPLEMENTATION. For GNSS satellites, this nominal signal model is well established. For 5G measurements, it depends on the work described in the previous section and the references cited therein. In an initial assessment, only pseudorange measurements from 5G are considered for the protection level computation. The obvious advantage is the analogy to GNSS measurements, limiting the algorithm's complexity.

Aside from the nominal measurement model, two prior fault probabilities need to be considered to compute protection levels. The first defines the probability of a single measurement to be faulty, in the scope of baseline ARAIM called P_{sat}. The second defines the probability of more than one measurement from a group of measurements to be faulty, in ARAIM called P_{const}. Faulty describes the event that the nominal measurement model is no longer valid.

While these probabilities are once again well characterized for GPS and are in the process of being explored for other GNSS, values are yet to be defined for 5G measurements. This is a considerable effort, involving the analysis of years of data. A good example of the complexity of such a characterization is shown by the effort conducted for GLONASS in Gunning, K., Walter, T., and Enge, P. (2017).

The GNSS receiver receives these prior probabilities and related ARAIM parameters through the Integrity Support Message (ISM). Similarly these values could be transmitted through a "5G ISM" message contained within the 5G navigation signal.

It further has to be noted that ARAIM is currently designed for the aviation user. The multipath and interference environments of this use case are relatively benign and well established multipath error models exist. Fault events of measurements not following the nominal model are mainly due to faults within the space segment. This is not the case for 5G measurements that are possibly used in an urban canyon. Multipath and even interference events might affect the fault probabilities aside from errors caused by the 5G tower or network. Within the scope of this study, preliminary values are set for the probabilities in the following section to explore the integrity gain under these circumstances. These are based on values determined for GNSS by efforts such as Gunning, K., Walter, T., and Enge, P. (2017) and Blanch, J., Liu, X., Gunning, K., and Walter, T. (2021) and summarized in Table 2.

TABLE 2

Summary of prior fault probabilities for GNSS

Parameter	GPS	GLONASS	Galileo	Beidou
P_{sat}	10^{-5}	10^{-4}	3×10^{-5}	10^{-5}
P_{const}	10^{-8}	10^{-4}	2×10^{-4}	6×10^{-5}

The implementation chosen within the HOP-5G testbed leverages on the openly accessible Stanford MAAST code from https://gps.stanford.edu/resources/software-tools/maast. The codebase represents a full Matlab System Volume Simulator (SVS) to analyze ARAIM performance. The code is expanded to allow for 5G measurements as an additional constellation, allowing for the use of the full hypothesis selection and protection level computation provided by the codebase.

PERFORMANCE ANALYSIS. The effect of adding 5G pseudorange measurements on the resulting PL is analyzed using real GNSS and simulated 5G measurements. Based on the previous literature results, the following values are set for the ARAIM parameters: $P_{const,5G} = 10^{-4}$ $P_{sig,5G} = 10^{-3}$, $\sigma_{5G} = 1\,m$, $b_{int,5G} = 0\,m$. To account for the more severe multipath environment likely encountered by 5G measurements, the prior probability of a single signal not adhering to the nominal measurement model $P_{sig,5G}$ has been increased tenfold compared to the most pessimistic GNSS constellation in Table 2, and by a factor of 100 compared to GPS. As common in integrity analysis, the results are condensed into the Horizontal Protection Level (HPL) and Vertical Protection Level (VPL). Only two scenarios are analyzed as showcase, using GPS and Galileo as baseline.

Integrity Scenario 1. The first scenario represents good working conditions for GNSS with an elevation mask angle of 15 degree and a healthy amount of satellites in view. Three 5G base stations are further in view. Figure 8 (left plot) shows the skyplot of the scenario. The 5G BS are located north, east and southwest of the user. The eastern BS is located at negative elevation, simulating a scenario of a UAV flying above the BS. Figure 8 (right plot) shows the Dilution of Precision (DOP) throughout the scenario. We can observe a moderate decrease in both VDOP and HDOP when adding 5G measurements. Thanks to the good GNSS conditions, both values had already been fairly low. The navigation error and PL are depicted in Figure 9. The plots show a similar result. The navigation error is comfortably below the PL at all times. Both are fairly low, corresponding to good GNSS conditions. The addition of 5G measurements only leads to a marginal improvement.

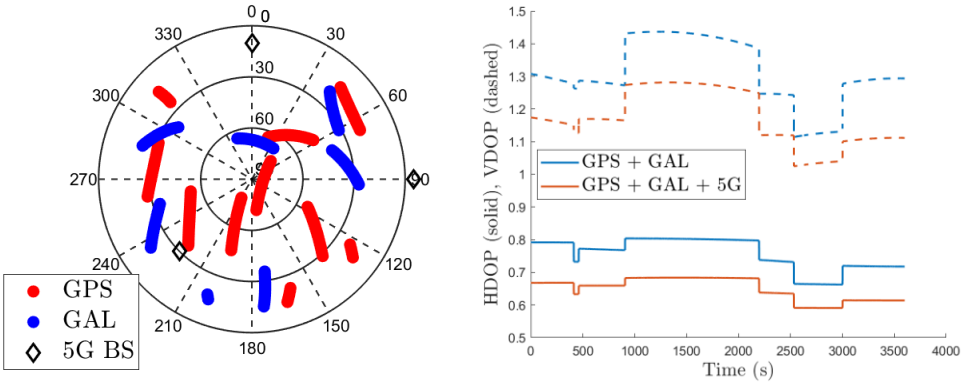

Figure 8 *Skyplot (left) and DOP (right) throughout integrity scenario 1*

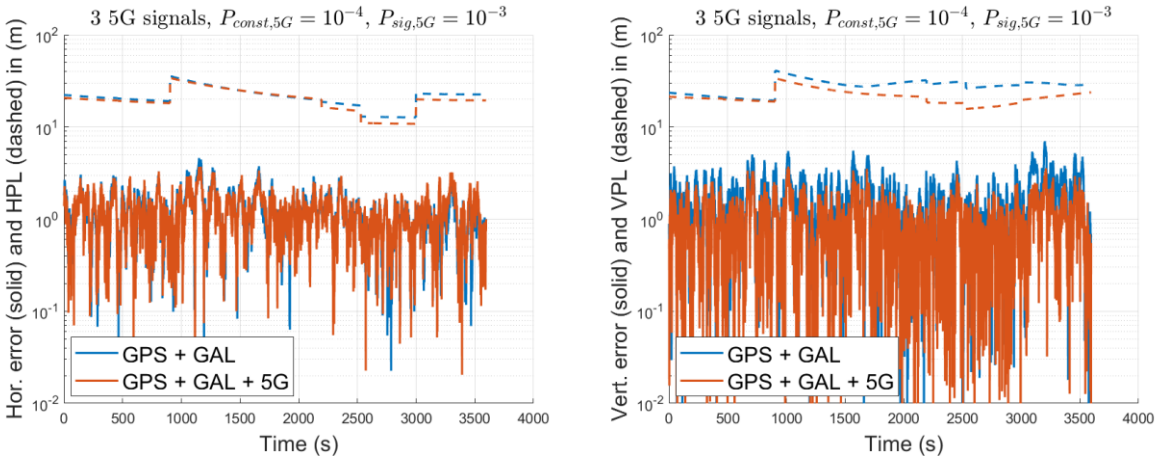

Figure 9 *Horizontal error and HPL (left) and vertical error and VPL (right) in integrity scenario 1*

Integrity Scenario 2. The second scenario now represents different circumstances. We use the ETSI urban canyon model as GNSS mask angle, simulating severe urban conditions ETSI (2015). The model mostly masks the eastern and western sections of the sky, reflecting a north-south oriented canyon. Four 5G BSs are now available, located northeast, southeast, southwest and northwest of the user. Two BSs (southeast and northwest) are below the horizon, once again representing a flying UAV user. Figure 10 (left plot) depicts the extreme conditions. Only a limited number of GNSS satellites are visible due to the severe masking. This is reflected in the DOP shown in Figure 10 (right plot). The blue GNSS-only lines indicate dramatic values, including a $\sim 250\ sec$ period of insufficient satellites to calculate any DOP (or position) at all. The addition of 5G measurements changes the situation noticeably. DOPs are reduced back down to low values, recovering the poor GNSS geometry.

A similar effect can be witnessed in the PL plots in Figure 11. The addition of 5G measurements visibly reduces the navigation error, making it almost independent of the volatile GNSS measurements.

Even more interesting is the PL result. The number of GPS measurements is insufficient to compute an integrity bound. The small number of satellites in view does not offer sufficient redundancy due to $P_{const,GAL}$ exceeding the allowed integrity risk. This changes at least during the first 800 sec with the addition of 5G signals. The extra signals now allow for a PL computation while a sufficient number of GNSS satellites is in view. After around 800 sec, the small number of satellites in view together with the conservative prior fault probabilities assigned to the 5G measurements does no longer enable us to compute an integrity bound.

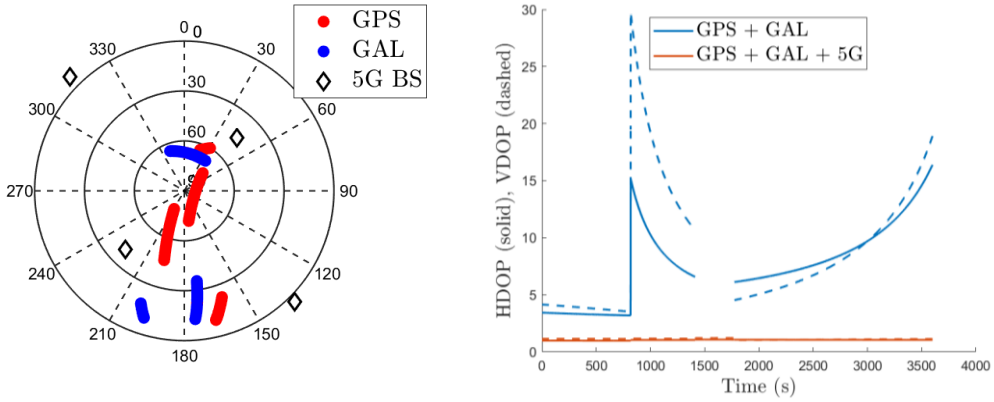

Figure 10 *Skyplot (left) and DOP (right) throughout integrity scenario 2*

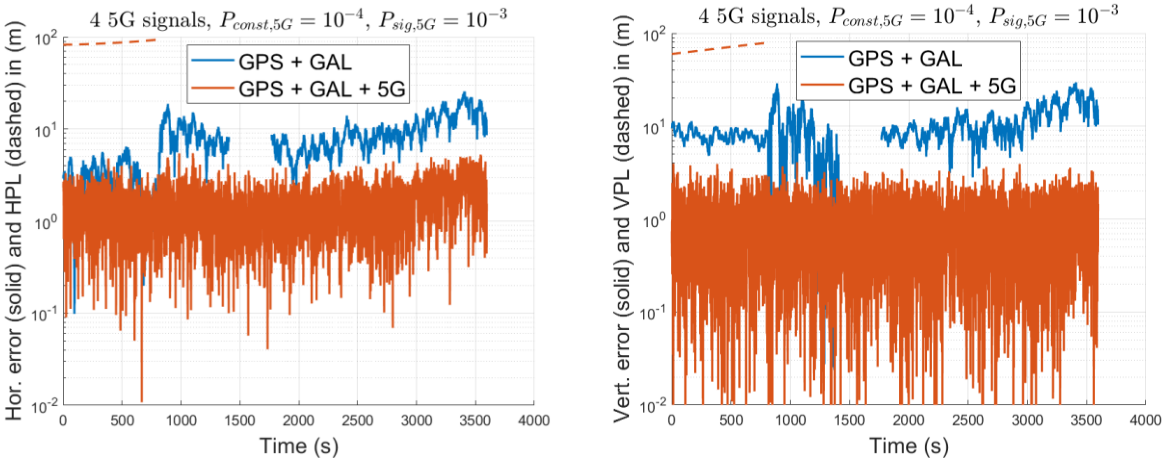

Figure 11 *Horizontal error and HPL (left) and vertical error and VPL (right) in integrity scenario 2*

4. EXPERIMENTAL LABORATORY RESULTS OF HOP-5G BS SYNCHRONIZATION

The results discussed in Sec. 3.2 remark the importance of the time synchronization between the 5G BSs, in order to achieve accurate positioning accuracies exploiting 5G signals, at least for TDoA-based positioning approaches. Within the HOP-5G testbed, the synchronization is supported through the usage of GNSS Disciplined Oscillator (GNSSDO), providing the PPS and 10 MHz signals to the SDR, with the 5G signal transmissions that are triggered at the pulses of the PPS signals.

This section evaluates the PPS accuracy of two GNSSDOs within the HOP-5G testbed, based on two experimental setups:

- **Jackson Labs GNSSDO**: The first setup is based on Jackson Labs Super Fury Desktop OCXO/DCXO GNSSDO, shortly GNSSDO. The Jackson Labs GNSSDO performances have been characterized through the setup depicted in Figure 12 (left). It makes use of live GNSS signals received by an antenna in open sky conditions. A signal splitter is used between the antenna and the GNSSDO, since a power supply is connected to the output of the splitter allowing the DC to pass, in order to supply power to the antenna. The GNSSDO is capable of internally estimating, with some delay, the time misalignment between its PPS and the PPS compatible with the received signal. Therefore, a laptop is connected to the GNSSDO in order to retrieve such time misalignment. It is worth to remark that the used antenna is a single frequency L1 antenna and the GNSSDO has been configured to process only GPS signals, hence it is working as a GPSDO.
- **Ettus Research GPSDO**: The second setup is based on Ettus Research TCXO/OCXO GPSDO add-on board. The performances of the board-mounted GPSDO by Ettus Research have been assessed through the setup illustrated in Figure 12 (right). It exploits a Spirent GSS6700 simulator for the generation of GPS signals that are sent through an RF cable of length 2 meters to the USRP X300 containing the GPSDO receiver. The PPS signal generated by both the Spirent and the USRP X300 (i.e., by the GPSDO) are acquired by an Oscilloscope through two RF cables of the same length (1 meter). The Oscilloscope generates data that are retrieved and processed by a laptop in order to assess the time misalignment between the GPSDO PPS and the Spirent PPS, which is considered as the reference.

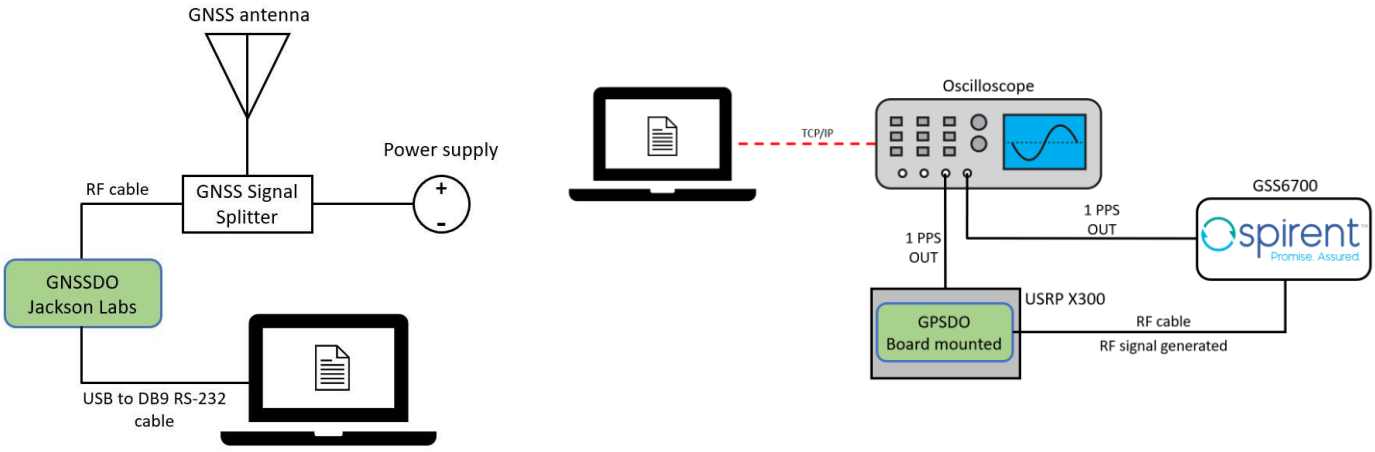

Figure 12 *Setup for the assessment of the GNSSDO PPS misalignment using signal in space (left) and of the GPSDO PPS misalignment using Spirent simulator*

4.1 EXPERIMENTAL RESULTS WITH JACKSON LABS GNSSDO SETUP

Figure 13 shows the PPS misalignment of the GNSSDO obtained during a specific test. An auto-survey of 2000 points has been configured, corresponding to about 2000 seconds, instead of the default value of 10000 points. Figure 13 (left) depicts the results after the GNSSDO has completed the auto-survey and has switched into locked status (about 15 minutes after the auto-survey has ended). The time misalignment is collected for 15 hours. During this time interval the achieved results are far from the 20 ns 1-sigma accuracy declared in the datasheet (datasheet specifications refer to a scenario after 3 days of operations with GPS reception in still air). Figure 13 (right) shows the time misalignment obtained in the subsequent 5 hours of the test, indeed Figure 13 (right) starts from the final value of Figure 13 (left). At this point about 16 hours have expired since the GNSSDO has been turned on. The performances significantly improve with respect to the previous 15 hours, they are now more aligned with the expected 20 ns accuracy.

In addition to the absolute misalignment error, another important metric to assess is the misalignment stability. Figure 14 (right) shows that, once the GNSSDO converges to a good solution, the time misalignment is still subject to some noise and a drift that is slowly corrected by the GNSSDO (several tens of minutes may pass before the drifts switches the sign). In order to remove the effect of the random noise a Simple Moving Average (SMA) filter is applied to the time misalignment, with a number of point equal to N=9. Since the time step of the data is 1 minute, using 9 points for the SMA means that the value at time t is computed by averaging the time misalignment at time t with the four time misalignments collected in the previous 4 minutes and with the four time misalignments collected in the subsequent 4 minutes.

Figure 14 (left) depicts the first derivative of the moving average of the time misalignment, representing an estimate of the time drift. This figure shows that the time drift can reach absolute values as large as 3 ns/min, corresponding to a pseudorange variation of almost 1 m/min, when the PPS is used to trigger the transmission of ranging signals. In order to assess how fast the time drift can vary, the derivative of the moving average of the time drift is computed, obtaining the second derivative of the time misalignment. The results, reported in Figure 14 (right), show that the time drift can change with a rate as large as 0.4 ns/min^2, in absolute value.

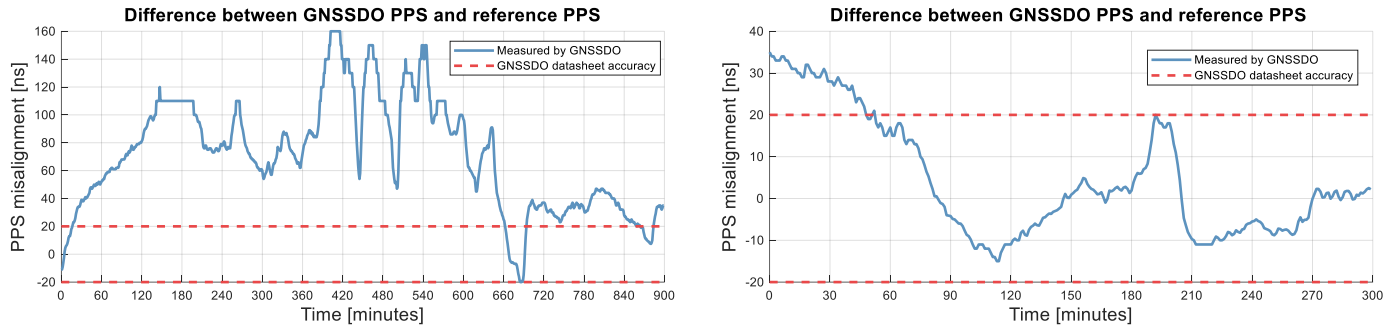

Figure 13 *PPS misalignment of GNSSDO after 45 minutes (left) and after 16 hours (right)*

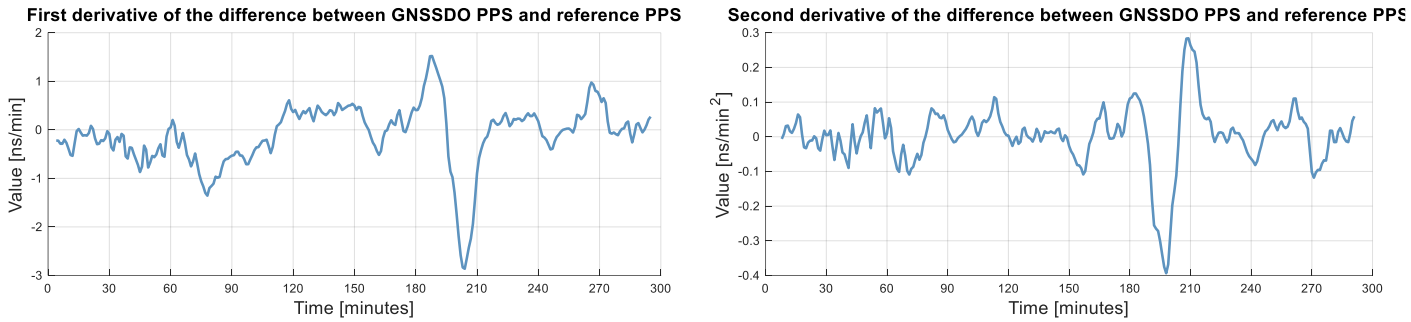

Figure 14 *First (left) and second (right) derivative of the PPS misalignment of GNSSDO after 16 hours*

4.2 EXPERIMENTAL RESULTS WITH ETTUS RESEARCH GPSDO SETUP

This experimentation assesses the PPS misalignment of the GPSDO obtained during a specific test. It is worth to remark that the results are impacted by the 2 meters RF cable connecting the Spirent with the GPSDO: the GPSDO tries to generate a PPS that is compatible with the received GPS signals, arriving $2/(3 \cdot 10^8) = 6.7$ ns later with respect to the transmitted ones. As a consequence, if the GPSDO were capable of generating a perfect PPS with respect to the received signals (no estimation error), because of the setup a positive error of 6.7 ns is measured by the oscilloscope. Thus, the results shown in Figure 15 include a compensation -6.7 ns with respect to the y-axis to correctly assess the GPSDO performance. The results in Figure 15 have been collected for 4 hours, starting 5 minutes after the GPSDO has been switched on and connected to the Spirent. The GPSDO converges quickly to values compatible to its declared accuracy of 50 ns (1-sigma), in less than 1 hour since it has been switched on, much quicker with respect to what observed for the Jackson Labs GNSSDO.

Initially the time misalignment changes often and sharply, it seems the GPSDO disciplines its clock often and with significant corrections. After 3 hours since the GPSDO has been switched on the time misalignment becomes more stable, suggesting it is correctly converging. These considerations are confirmed by Figure 16 (left) and Figure 16 (right), depicting respectively the first and second derivative of the moving average of the time misalignment (as for the GNSSDO tests, the moving average is such that the value at time t is computed by averaging the time misalignment at time t with the misalignments collected in the previous and subsequent 4 minutes). The values of these derivatives after 3 hours since the GPSDO has been switched on significantly decrease, in absolute value, with respect to those observed in the first 3 hours.

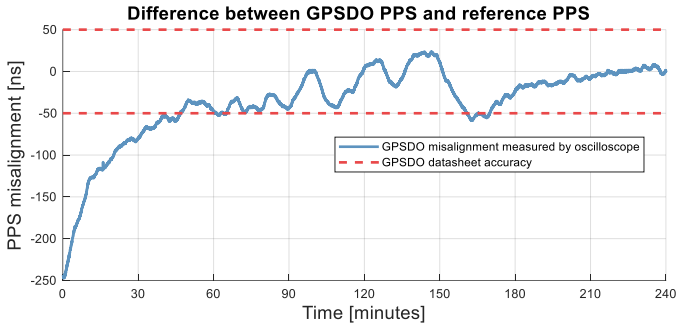

Figure 15 *PPS misalignment of GPSDO after 5 minutes*

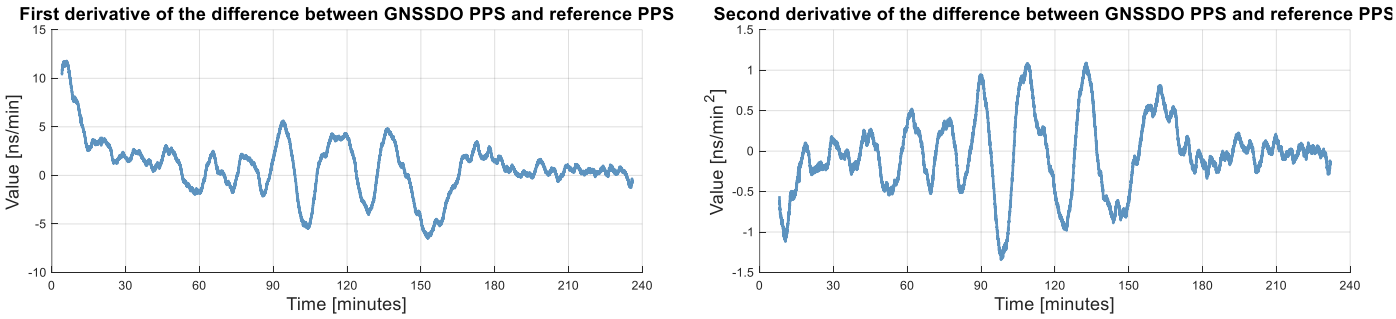

Figure 16 *First (left) and second (right) derivative of the PPS misalignment of the GPSDO after 5 minutes*

5. CONCLUSIONS

This paper provides first simulation and experimental results of a proof-of-concept of dedicated aerial hybrid 5G and GNSS testbed. The simulation results assess the key performance factors on User Equipment (UE) positioning within the HOP-5G testbed. Among these factors, the base station (BS) network synchronization has a significant impact on the downlink time-difference of arrival (DL-TDoA), which is mainly considered in the HOP-5G testbed. In addition, the potential improvement in realistic integrity bounds are explored under an initial measurement model with the fusion of real GNSS and simulated 5G measurements, indicating the benefits of 5G with a reduced GNSS satellite availability. Finally, extensive experimental results on the BS synchronization are provided, in order to assess their impact in the final accuracy of DL-TDoA. The results concerning the achievable PPS accuracy of the GNSSDOs suggest the usage of a monitoring unit for the time offset estimation of the 5G BSs. Future field results are expected to provide further insights on the hybrid fusion of GNSS, 5G and sensors for UE positioning.

ACKNOWLEDGMENTS

This work from the Hybrid Overlay Positioning with 5G and GNSS (HOP-5G) project has been supported by the European Space Agency Navigation Innovation and Support Programme (NAVISP), which aims to generate innovative concepts, technologies and system solutions in the wide-field of Positioning, Navigation and Time.

REFERENCES

3GPP TR 22.872 (2018). Study on positioning use cases. Release 16.

3GPP TR 38.857 (2021). Study on NR positioning enhancements. Release 17.

3GPP TR 38.855 (2019). Study on NR positioning support. Release 16.

3GPP TS 38.305 (2020). NG-RAN; Stage 2 functional specification of User Equipment (UE) positioning in NG-RAN. Release 16.

3GPP TS 38.901 (2019). Study on channel model for frequencies from 0.5 to 100 GHz. Release 16.

Abdallah, A. & Kassas, Z. (2021). UAV navigation with 5G carrier phase measurements. *Proc. ION GNSS+ 2021*.

Blanch, J., Liu, X., Gunning, K., and Walter, T. (2021). Analysis of GNSS Constellation Performance for Advanced RAIM. In *Proceedings of the 34th International Technical Meeting of the Satellite Division of The Institute of Navigation (ION GNSS+ 2021)*, pages 1410–1434, St. Louis, Missouri

Blanch, J. and Walter, T. (2021). A Fault Detection and Exclusion Estimator Designed for Integrity. In *Proceedings of the 34th International Technical Meeting of The Satellite Division of the Institute of Navigation (ION GNSS+ 2021)*, pages 1672–1686, St. Louis, Missouri.

Blanch, J., Walter, T., Enge, P., Lee, Y., Pervan, B., Rippl, M., Spletter, A., and Kropp, V. (2014). Baseline Advanced RAIM User Algorithm and Possible Improvements. *IEEE Transactions on Aerospace and Electronic Systems*, 51(1):713–732.

Blanch, J., Walter, T., Milner, C., Joerger, M., Pervan, B., and Bouvet, D. (2022). Baseline Advanced RAIM User Algorithm: Proposed Updates. In *Proceedings of the 2022 International Technical Meeting of The Institute of Navigation*, pages 229–251.

del Peral-Rosado, J.A. et al. (2017). Evaluation of Hybrid Positioning Scenarios for Autonomous Vehicle Applications. *Proc. ION GNSS+ 2017*.

del Peral-Rosado, J. A., Raulefs, R., López-Salcedo, J. A., Seco-Granados, G. (2018a). Survey of cellular mobile radio localization methods: From 1G to 5G. *IEEE Commun. Surveys Tuts.*, 20 (2), 1124-1148.

del Peral-Rosado, J.A., Saloranta, J., Destino, G., López-Salcedo, J.A., Seco-Granados, G. (2018b). Methodology for Simulating 5G and GNSS High-Accuracy Positioning. *Sensors*, 18, 3220.

del Peral-Rosado, J.A. et al. (2019). Physical-Layer Abstraction for Hybrid GNSS and 5G Positioning Evaluations. *Proc. VTC2019-Fall*.

del Peral-Rosado, J. A. et al. (2022). Design Considerations of Dedicated and Aerial 5G Networks for Enhanced Positioning Services. *Proc. NAVITEC*.

Dwivedi, S. et al. (2021). Positioning in 5G networks. *IEEE Commun. Mag.*, 59(11), 38-44.

ETSI TS 103 246-3 (2015). Satellite Earth Stations and Systems (SES); GNSS based location systems; Part 3: Performance requirements

Gunning, K., Blanch, J., Walter, T., de Groot, L., and Norman, L. (2018). Design and evaluation of integrity algorithms for PPP in kinematic applications. In *Proceedings of the 31st International Technical Meeting of the Satellite Division of the Institute of Navigation, ION GNSS+ 2018*, pages 1910–1939, Miami, Florida

Gunning, K., Walter, T., and Enge, P. (2017). Characterization of GLONASS broadcast clock and ephemeris: Nominal performance and fault trends for ARAIM. In *Proceedings of the 2017 International Technical Meeting of The Institute of Navigation, ITM 2017*, pages 170–183.

Joerger, M. and Pervan, B. (2013). Kalman filter-based integrity monitoring against sensor faults. *Journal of Guidance, Control, and Dynamics*, 36(2):349–361

Joerger, M. and Pervan, B. (2016). Exploiting Satellite Motion in ARAIM: Measurement Error Model Refinement Using Experimental Data. In *29th International Technical Meeting of the Satellite Division of the Institute of Navigation, ION GNSS 2016*, pages 1696–1712.

Maaref, M., Khalife, J., and Kassas, Z. M. (2021). Aerial Vehicle Protection Level Reduction by Fusing GNSS and Terrestrial Signals of Opportunity. *IEEE Transactions on Intelligent Transportation Systems*, 22(9):5976–5993.

Mata, F.J. et al. (2020). Preliminary field trials and simulations results on performance of hybrid positioning based on GNSS and 5G signals. *Proc. ION GNSS+ 2020*.

Maymo-Camps, R. et al. (2018). 5G positioning and hybridization with GNSS observations. *Proc. ITSNT*.

Parkinson, B. W., & Axelrad, P. (1988). Autonomous GPS Integrity Monitoring Using the Pseudorange Residual. *Navigation*, 35 (2), 255–274. doi: 10.1002/j.2161-4296.1988.tb00955.x

RP-213588 (2021). Revised SID on Study on expanded and improved NR positioning. *3GPP TSG RAN Meeting #94e*.

Shamaei, K., & Kassas, Z.M. (2021). Receiver Design and Time of Arrival Estimation for Opportunistic Localization With 5G Signals. *IEEE Trans. Wireless Commun.*, 20(7), 4716-4731.

Wendel, J. (2016). An Efficient Filter Bank Approach for the Provision of Integrity in Integrated Navigation Systems. In European Journal of Navigation